II. MICROWAVE GASEOUS DISCHARGES

Prof. S. C. Brown
Prof. W. P. Allis
Dr. K. S. W. Champion
Helen R. Land
J. J. McCarthy
G. J. Schulz

A. HIGH-DENSITY MICROWAVE GASEOUS DISCHARGES

As described in a previous report (1) there are two types of plasma resonance. The first, impedance resonance, occurs when $|E/J|$ has a maximum value. The second occurs when the dielectric constant k_r is zero. This type of resonance will now be termed dielectric resonance. In Fig. II-1 are plotted curves giving the density at the center of a discharge corresponding to impedance resonance or dielectric resonance at the center and $(\pi\Lambda)/10$, $(\pi\Lambda)/25$, and $(\pi\Lambda)/100$ from the wall, respectively. The curves were calculated for discharges between two extended plane parallel plates and are accurate to within 5 percent when the discharge diameter is greater than 4.8 times its height.

To calculate the curves for resonance near the walls, it was necessary to make use of the appropriate electron density distributions. For high pressures or densities the distributions given in Figs. 2 and 3, respectively, of Allis, Brown, and Everhart (2) were used. However, at lower pressures the distribution varies continuously from the high-pressure curves to those in Fig. 4 (ibid.) which are typical for intermediate pressures to those in Fig. II-2, which represent the low-pressure limit for the density distribution. When $a = 2$ (where a is the exponent in the expression for ν_i) the relation for ℓ, the distance from the wall at which the density corresponds to impedance resonance, is simply

$$\ell = \frac{\pi\Lambda}{2\left[1 + L_o r_o \left(r_o^2 - 1\right)^{1/2}\right]}$$

where $L_o^2 = \frac{\pi\omega^3}{\nu_c^3}$, and r_o is the density at the center of the discharge (in normalized units such that $r = 1$ at impedance resonance). It is obvious from this expression that when $\nu_c \to 0$, $\ell \to 0$ as the low-pressure limit.

Double probes were used to measure the density of charged particles in 3 Mc/sec discharges in 2 mm of hydrogen. With densities of 10^9-10^{10} electrons/cm^3, the discharge had the usual appearance expected above plasma resonance. However, with densities a little below 10^8 electrons/cm^3, the interior of the discharge appeared uniformly bright, the edges being a little less luminous. This discharge had an appearance that was believed only possible below plasma resonance, but the observed density was almost 10^3 times that for impedance resonance under these conditions.

Re-examination of the theory showed that, indeed, this phenomenon was to be expected when $p\lambda$ was large. The basic expression for the impedance of a discharge may be

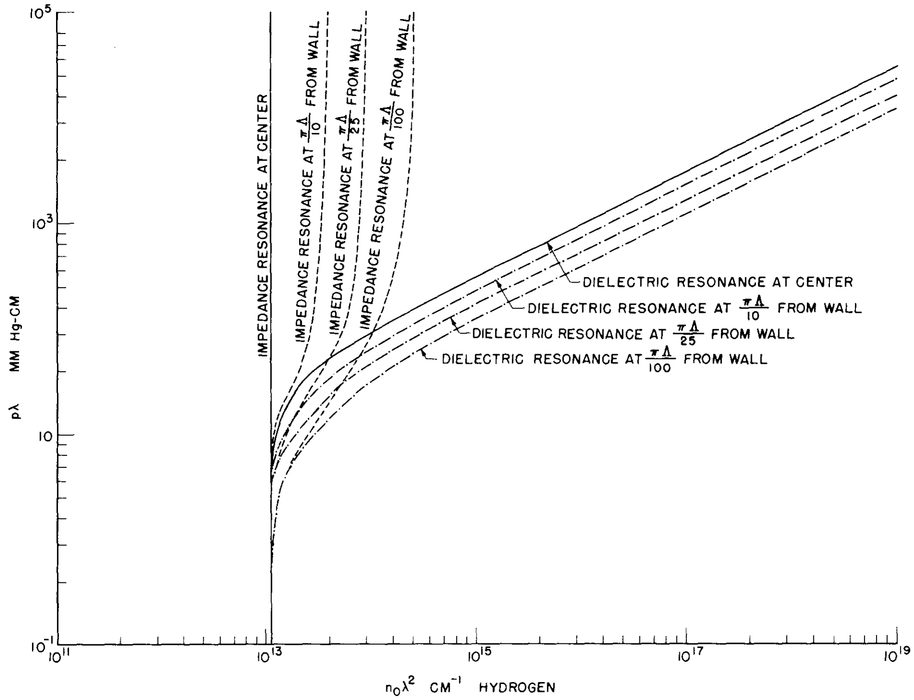

Fig. II-1

Plasma resonance boundaries in hydrogen. The curves give the conditions for impedance resonance and dielectric resonance, respectively, to occur at the center of a discharge and at specified distances from the walls. The values were calculated for discharges whose diameter ≥ 4.8 height and with $\alpha = 2$.

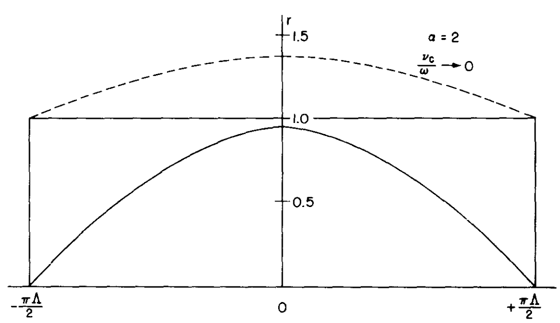

Fig. II-2

The low-pressure limit of the distribution of electron density across a discharge. For central densities below plasma resonance the curve is a cosine. With higher densities the distribution changes and tends, as an upper limit, to the rectangular curve for which r = 1. Distributions such as the dotted curve can also be obtained from the equations but are impossible to produce because of the limitations of dielectric resonance.

written

$$\left|\frac{E}{J}\right| = \frac{\left[1 + \left(\frac{\nu_c}{\omega}\right)^2\right]^{1/2}}{\omega\epsilon_o\left[(r-1)^2 + \left(\frac{\nu_c}{\omega}\right)^2\right]^{1/2}}$$

$$= \frac{\left[1 + \left(\frac{\nu_c}{\omega}\right)^2\right]^{1/2}}{\nu_c\epsilon_o\left[1 + \left(\frac{r-1}{\nu_c/\omega}\right)^2\right]^{1/2}}$$

$$\approx \frac{1}{\nu_c\epsilon_o}\left[1 + \left(\frac{\nu_c}{\omega}\right)^2\right]^{1/2}\left[1 - \frac{1}{2}\left(\frac{r-1}{\nu_c/\omega}\right)^2 + \ldots\right]$$

when $|r-1|$ is small. Set $r = 1 \pm \delta r$, then

$$\left|\frac{E}{J}\right| \approx \text{const}\left[1 - \frac{(\delta r)^2}{2(\nu_c/\omega)^2}\right]$$

From this relation it can be seen that in the vicinity of $r = 1$ the plot of $|E/J|$ as a function of r is a portion of an inverted parabola with maximum at $r = 1$. When ν_c/ω is small, $|E/J|$ falls off extremely rapidly on either side of the maximum, but when ν_c/ω is large, $|E/J|$ is essentially constant for relatively large changes in r. In Fig. II-3 is plotted $|E/J|$ at the center of a discharge as a function of the central density for a typical high-pressure case. Thus it can be seen that if the density at the center of the discharge is such that $|E/J|$ is in the approximately constant region, the discharge will appear the same as one below plasma resonance. In fact, discharges above plasma resonance can take several different forms. These can be predicted by calculations such as those yielding Fig. II-4. In Fig. II-4 are plotted lines giving the densities at which the E-field at the center, $(\pi\Lambda)/10$, $(\pi\Lambda)/25$, and $(\pi\Lambda)/100$, respectively, are 5 percent below the maximum value of the E-field (impedance resonance) for the same $p\lambda$. Obviously there is one set of curves above resonance and another below. If the density at the center of a discharge and p and λ are specified the appearance of the discharge can be predicted from Fig. II-4. This is not only qualitative but also quantitative. For example, the thickness of bright layers (where present) can be deduced. It is planned to carry out a systematic set of experiments to determine whether or not

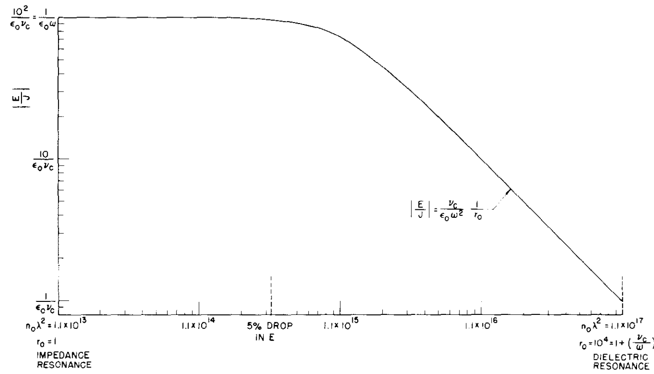

Fig. II-3

Values of $|E/J|$ at the center of a discharge as a function of $n_o\lambda^2$ for a typical high-pressure case $(\nu_c/\omega) = 100$. The value of $|E/J|$ at impedance resonance is $\left[1 + (\nu_c/\omega)^2\right]^{1/2}/\epsilon_o \nu_c$, which approximately equals $1/\epsilon_o \omega$ at high pressures. Near dielectric resonance $|E/J| = \nu_c/\epsilon_o \omega^2 r$ and hence falls off linearly to the limiting value $1/\epsilon_o \nu_c$. Thus the ratio of the values of $|E/J|$ at the two resonances is $\left[1 + (\nu_c/\omega)^2\right]^{1/2}$, which approximately equals ν_c/ω at high pressures.

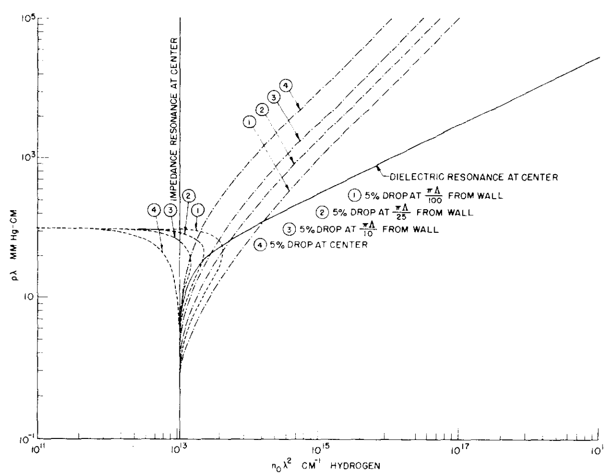

Fig. II-4

Curves giving the values of $n_o\lambda^2$ at which $|E/J|$ is 5 percent less, at the center, $(\pi\Lambda)/10$, $(\pi\Lambda)/25$, and $(\pi\Lambda)/100$, respectively, than the maximum value of $|E/J|$ for the same $p\lambda$. The value of $|E/J|$ falls off, of course, on both sides of impedance resonance.

the detail of the theory can be verified.

K. S. W. Champion

References

1. Quarterly Progress Report, Research Laboratory of Electronics, M. I. T., October 15, 1953, pp. 7-9.

2. W. P. Allis, S. C. Brown, and E. Everhart, Phys. Rev. 84, 519 (1951).

B. PROBE STUDIES

The microwave cavity with probe assembly, described in the Quarterly Progress Report, October 15, 1953 (shown in Fig. II-5 of that report), was used to study the low-pressure behavior of the positive ion saturation current to probes. At very low pressures the ions entering the sheath will describe orbital motions around the probes (1). Approximating the functions entering this theory by analytical expressions, the following expression was obtained for the positive ion current, i, arriving at the probe

$$i = C_1 n^{0.8} V^{0.555}$$

where n is the positive ion density, V is the probe-to-plasma potential, and C_1 is a parameter depending on probe size, electron energy, and gas. This equation will break down in two cases:

1. When the pressure becomes high enough so that the positive ion makes, on the average, one or more collisions in the sheath, it will be removed from its orbital motion. Because the field is high in the sheath the ion will reach the probe. When at least one collision occurs in the sheath practically all of the ions reaching the sheath edge will be collected by the probe.

2. When applied potentials are high, practically all of the ions will again reach the probe.

When conditions 1 and 2 are applicable, it is better to assume that all of the ions reaching the sheath will be collected by the probe. The equation governing this case is

$$i = C_2 n^{0.578} V^{0.633}$$

where C_2 is again a parameter depending on gas, electron energy, and probe size. In this equation, the β-function entering the solution of the Child-Langmuir equation in cylindrical coordinates was approximated by an analytical expression. Figures II-5 and II-6 show the experimental results. The values for electron densities were obtained by microwave measurements. If we refer to Fig. II-5 we can see that the slope of 0.55, characteristic of orbital motion, persists to potentials that decrease as the density

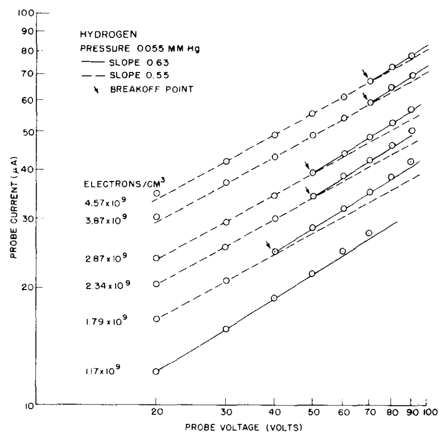

Fig. II-5

Saturated positive ion probe current vs probe voltage at 0.055 mm Hg in hydrogen.

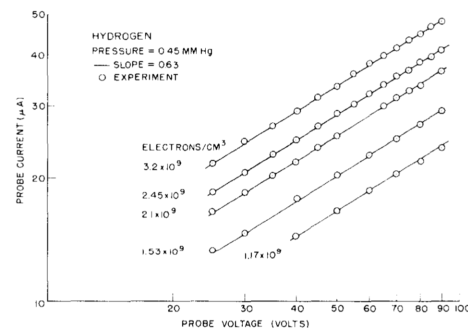

Fig. II-6

Saturated positive ion probe current vs probe voltage at 0.45 mm Hg in hydrogen.

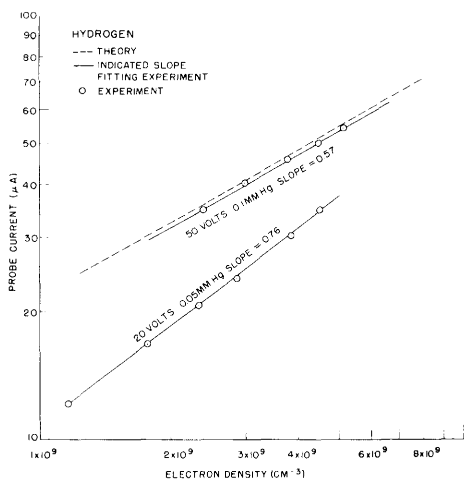

Fig. II-7

Saturated positive ion probe current vs electron density at specified voltage and pressure in hydrogen.

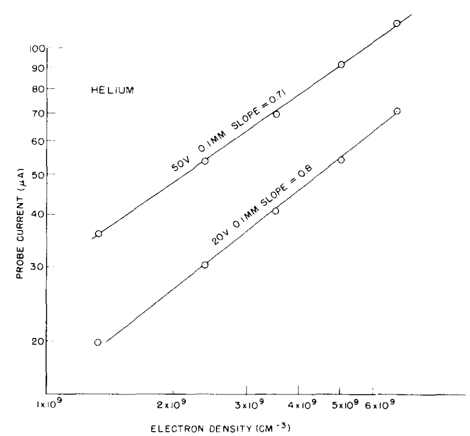

Fig. II-8

Saturated positive ion probe current vs electron density in helium.

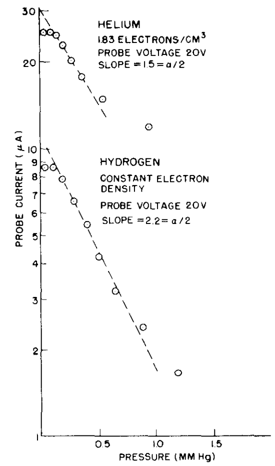

Fig. II-9

Probe current vs pressure in helium and hydrogen.

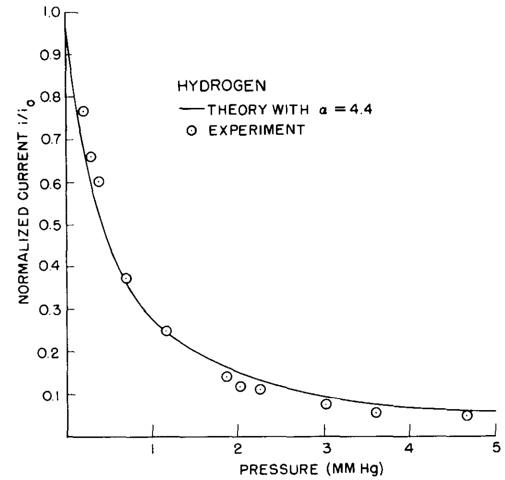

Fig. II-10

Normalized saturated positive ion current vs pressure at constant probe voltage and electron density in hydrogen.

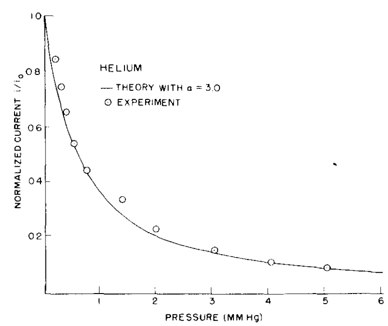

Fig. II-11

Normalized saturation positive ion current vs pressure at constant probe voltage and electron density in helium.

decreases. However, a decrease in density means an increase in sheath size and therefore a larger probability of making collisions within the sheath. At low densities the line has a slope of 0.63, characteristic of nonorbital motion. Figure II-6 shows that at higher pressures (0.45 mm Hg) all the curves have a slope of 0.63 because of the many collisions in the sheath.

Further check for the two equations comes from a plot of i vs n. Figure II-7 shows that the slopes are in agreement with theory. Figure II-8 shows that the transition to nonorbital motion in helium occurs at higher pressure. The reason for this is the lower collision probability for positive ions in helium, which increases the mean-free path. As the pressure is further increased, the current to the probe will decrease at constant plasma density of ions and at constant probe potential because a reflected current is set up by multiple collisions. Eventually, mobility will be the controlling factor.

An approximate theory for the transition from low-pressure probe currents to mobility-controlled currents yields the following expression for the probe current

$$i = \frac{i_o}{2} \frac{3 - \exp(-a p)}{1 + a p} \quad \text{(at constant ion density and probe voltage)}$$

where i_o is the current at $p \to 0$, and a is a function of the collision probability, P_c, and the sheath size, S; that is,

$$a = P_c S$$

The parameter a can be determined experimentally from the equation given above by noting that

$$\left. \frac{d \ln i}{dp} \right|_{p \to 0} = -\frac{a}{2}$$

The evaluation of a is shown in Fig. II-9 for helium and hydrogen. Figures II-10 and II-11 show a plot of the theoretical expression in the form of i/i_o vs p together with experimental points taken at constant density of ions (as monitored by the microwave measuring signal) and constant probe voltage.

G. J. Schulz

References

1. H. M. Mott-Smith and I. Langmuir, Phys. Rev. 28, 727 (1926).

C. MICROWAVE BREAKDOWN IN HYDROGEN AT HIGH PRESSURES

Work on the continuous-wave microwave breakdown in hydrogen has been completed. The main purpose of this work was to study still further the anomalous departure of experiment and theory near values of p/E of 0.11 that was observed in the work done (1) at 100 Mc/sec and in the work done (2) at 3000 Mc/sec.

Three resonant cavities of 10.6-cm wavelength and varying in height from 1/8 inch to 1/2 inch were constructed of oxygen-free, high-conductivity copper. Varying the height of the cavities enabled us to check the dependence of breakdown on the diffusion length of the cavity. The housekeeper type of coupling loop window of the earlier cavities was replaced by a modified Kovar-to-glass seal window which permitted the baking of the cavity at high temperatures in a hydrogen atmosphere without danger of destroying the seals. These windows are similar to the conventional type except that a copper sleeve extends in beyond the seal to shield it from the microwave power. Five sources of hydrogen were used: hydrogen obtained from a palladium tube heated in an atmosphere containing hydrogen; fresh, spectroscopically pure Airco hydrogen; old, spectroscopically pure Airco hydrogen; hydrogen obtained from thermal decomposition of uranium hydride prepared in the vacuum system previous to the experiment; and hydrogen taken directly from a tank of commercial grade hydrogen.

The data on the breakdown of hydrogen obtained from a palladium leak have been reported (2). They exhibited the anomalous behavior mentioned earlier. The data on the breakdown of bottle hydrogen were inconclusive because a sufficiently high pressure could not be reached to determine definitely whether or not the disagreement existed for this type of hydrogen. However, it should be mentioned that the data of the fresh sample of spectroscopically pure hydrogen were in agreement with previous data as far as they could be taken, but the data of the old sample were everywhere in considerable disagreement with theory and experiment and can only be attributed to impurities in this sample. Data obtained from tank hydrogen were in substantial agreement with earlier reported data and exhibited an increasing departure from theory for increasing values of p/E. Of all the data taken, only the data taken with hydrogen evolved from UH_3 by thermal decomposition (3) showed no increasing departure from theory for increasing values of p/E. It is reasonable to assume that this sample of hydrogen was quite pure. This fact would lend weight to the theory that the anomalous behavior noted in previous experiments must have been due to presence of impurities in the gas sample.

Some comments should be made on the effect of diffusion length or cavity size on the results of this experiment. The theory as calculated holds only for the case of uniform electric field or infinite parallel plate cavity. This condition is quite easily realized in the 100 Mc/sec cavity where the data follow the theory up to the point of the anomalous departure. However, in the microwave cavities, the condition of uniform electric field is not too well realized — the greater the height of the cavity, the more the data departed from the theory. Correcting the data by the method of Brown and Herlin (4), which was used successfully for air and Heg gas (5) in the case of nonuniform fields, yielded only about 50 percent of the desired correction. The fact that this method of correction for nonuniform field does not work well for hydrogen has been observed by others (5).

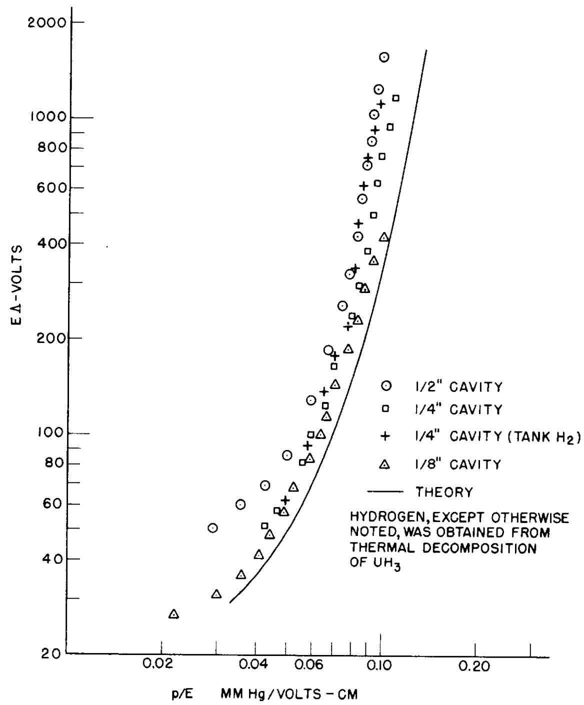

Fig. II-12

Hydrogen, except otherwise noted, was obtained from thermal decomposition of UH_3.

Figure II-12 shows that a plot of the experimental data obtained from pure hydrogen is parallel to the theory, and it may be concluded that there is no anomalous behavior in hydrogen obtained from UH_3.

Before taking any data on a cavity the vacuum system was pumped and baked for more than a week. The baking was done both in vacuum and in the presence of 5-10 cm of hydrogen. The ultimate pumping pressure was less than 10^{-8} mm Hg, as observed on a laboratory ionization gauge; the holding pressure was $2\text{-}4 \times 10^{-8}$ mm Hg after several hours.

J. J. McCarthy

References

1. Quarterly Progress Report, Research Laboratory of Electronics, M.I.T., April 15, 1952, p. 10.
2. Ibid., April 15, 1953, pp. 9, 10.
3. Ibid., pp. 13, 14.
4. M. A. Herlin and S. C. Brown, Phys. Rev. 74, 1650 (1948).
5. Quarterly Progress Report, Research Laboratory of Electronics, M.I.T., Jan. 15, 1952, pp. 8-11.